

## Article

# Microstructure and Oxidation Behavior of CrAl Laser-Coated Zircaloy-4 Alloy

Jeong-Min Kim <sup>1,\*</sup>, Tae-Hyung Ha <sup>1</sup>, Il-Hyun Kim <sup>2</sup> and Hyun-Gil Kim <sup>2</sup>

<sup>1</sup> Department of Advanced Materials Engineering, Hanbat National University, 125 Dongseo-daero, Yuseong-gu, Daejeon 34158, Korea; htman15@naver.com

<sup>2</sup> Light Water Reactor Fuel Technology Division, Korea Atomic Energy Research Institute, 989-111 Daedeok-daero, Yuseong-gu, Daejeon 34057, Korea; s-weat@hanmail.net (I.-H.K.); hgkim@kaeri.re.kr (H.-G.K.)

\* Correspondence: jmk7475@hanbat.ac.kr; Tel.: +82-42-821-1235

Academic Editor: Hugo F. Lopez

Received: 24 October 2016; Accepted: 10 February 2017; Published: 15 February 2017

**Abstract:** Laser coating of a CrAl layer on Zircaloy-4 alloy was carried out for the surface protection of the Zr substrate at high temperatures, and its microstructural and thermal stability were investigated. Significant mixing of CrAl coating metal with the Zr substrate occurred during the laser surface treatment, and a rapidly solidified microstructure was obtained. A considerable degree of diffusion of solute atoms and some intermetallic compounds were observed to occur when the coated specimen was heated at a high temperature. Oxidation appears to proceed more preferentially at Zr-rich region than Cr-rich region, and the incorporation of Zr into the CrAl coating layer deteriorates the oxidation resistance because of the formation of thermally unstable Zr oxides.

**Keywords:** laser coating; Zircaloy-4; CrAl; microstructure; oxidation

## 1. Introduction

Zirconium alloys have been widely used as nuclear materials because of their high chemical stability under the normal operating conditions of a pressurized or boiling water reactor, low absorption cross-section of thermal neutrons, and fairly good mechanical properties. However, Zr alloys are vulnerable to the high temperature oxidation that can occur in the case of accidents. Since explosive hydrogen is formed by the rapid zirconium oxidation, a reduced oxidation rate of Zr alloys at high temperatures is necessary to improve the accident tolerance [1–4]. As a short-term solution to the problem, protective coating through an efficient and economical method such as laser coating and thermal spray can be considered [2,4].

It has been previously reported that a laser coating of chromium on Zircaloy-4 cladding tube could enhance the high-temperature oxidation resistance significantly [2]. The diffusion of oxygen into the Zr substrate was observed to be effectively restricted by the Cr coating layer during the oxidation. When a coated alloy is exposed to a high temperature, a significant diffusion and microstructural variation may occur at the coating/substrate interface, even for a short time. In the case of laser-treated FeCrAl-coating on Mo alloy, an interfacial reaction was found to occur at high temperature [5].

Meanwhile, it was reported that Cr–Al composite coatings were very effective in enhancing the oxidation resistance of metals at high temperatures [6]. Since  $\text{Al}_2\text{O}_3$  and  $\text{Cr}_2\text{O}_3$  can form on the surface of Cr–Al coated alloys, the high temperature oxidation resistance is expected to increase even further. Although the superiority of Cr–Al laser coating has already been demonstrated, research on the stability of the microstructure at high temperature is not yet sufficient. In the case of Cr-coated Zr alloy, comparatively a few phases can be formed between Cr coating layer and Zr substrate according to the Zr–Cr binary phase diagram [7]. However, in the case of CrAl-coated Zr alloy, more complicated

interfacial reactions would occur during the solidification and when it is exposed to high temperatures. Therefore, in the present research, CrAl laser-coated Zr alloys were exposed to high temperatures, and then their microstructural variation and oxidation behavior were investigated.

## 2. Materials and Methods

Zircaloy-4 alloy (Zr-1.38%Sn-0.2%Fe-0.1%Cr, wt. %) sheets were used as the substrate, and CrAl (30 wt. % Al) coating layer with the average thickness of about 300  $\mu\text{m}$  was deposited on the surface of the Zr alloy through a laser coating process. A photograph of the laser equipment for coating is shown in Figure 1. The laser coating was carried out by using a continuous wave (CW) diode laser (wavelength of 1062 nm) with a maximum power of 300 W (PF-1500F model; HBL Co., Daejeon, Korea) and a power supply (Pwp14Y04K model; Yesystem Co., Daejeon, Korea). Coating process variables such as laser power, powder injection speed, specimen moving velocity, and gas flow speed were adjusted based on previous research results [8]. The applied power for the laser treatment ranged up to 300 W, and the scanning speed was 14 mm/s. To prevent any oxidation during the process, an inert gas (Ar) was continuously blowing into the melted surface of specimen. The mean size of the CrAl alloy powders as a raw material for coating was 90  $\mu\text{m}$ .

As previously mentioned, when used for nuclear fuel claddings or the like, it can be accidentally exposed to a high temperature for a long time, and it is presumed that the atmosphere is mainly water vapor. For ease of experiment, firstly, microstructural variations of the laser-coated specimens were investigated under argon or air atmosphere at 1100  $^{\circ}\text{C}$  for different holding times. Then, oxidation test of the CrAl and CrAlZr alloys was conducted in the steam atmosphere at 1200  $^{\circ}\text{C}$  for 1 h. Cr-30 wt. % Al and Cr-30 wt. % Al-20 wt. % Zr alloy specimens were prepared through vacuum arc remelting process to directly investigate the characteristics of the coating layers without Zr substrate. Microstructural analyses were performed using SEM (JEOL, Tokyo, Japan) equipped with an energy dispersive X-ray spectrometer (EDS, JEOL, Tokyo, Japan), and an X-ray diffractometer (XRD, Rigaku, Tokyo, Japan).

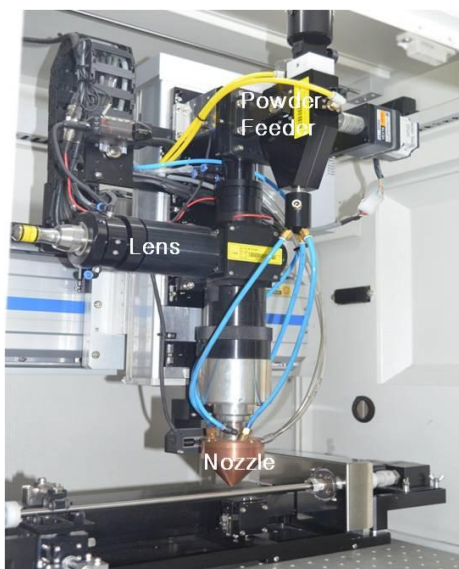


Figure 1. Appearance of the laser equipment for coating.

## 3. Results and Discussion

### 3.1. Microstructure of CrAl Laser-Coated Zr Alloy

Figure 2 shows SEM micrographs of CrAl laser coating layers on Zircaloy-4 alloy. Some Zr content could be measured in the CrAl coating layer that is far away from the Zr substrate (sometimes even near the coating surface), implying that significant intermixing of CrAl coating and Zr substrate

occurred during the laser coating. The light bottom area is Zr substrate, and the Zr content is increased as distance from the substrate is increased. A Zr-rich region appears between the Zr substrate and the CrAl coating layer. The composition of the Zr-rich part indicates the formation of a solid solution of Cr and Al in Zr. As indicated in Figure 2b, the majority of the Cr-rich coating layer is composed of two rapidly solidified regions: Cr-rich and AlZr(Cr) phases.

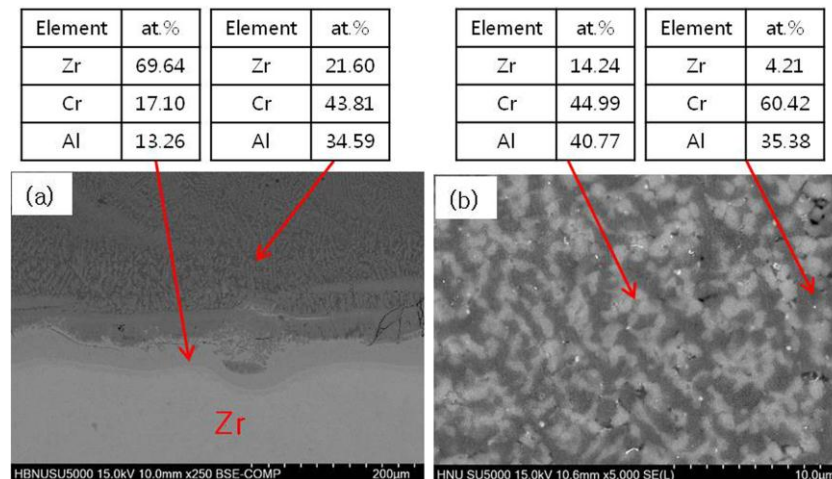


**Figure 2.** SEM-EDS (scanning electron microscopy–energy dispersive X-ray spectrometry) analysis results of CrAl laser-coated Zircaloy-4 substrate alloy: (a) near the Zr substrate; (b) Cr-rich coating layer.

If the mixture of CrAl coating powders and the top surface of substrate were completely melted and homogeneous, primary Cr phase would be formed first from the liquid, since the major component of the surface liquid pool was Cr. Normal solidification reactions to form phases for Cr-30 wt. % Al-20 wt. % Zr alloy (approximate chemical composition for the majority of the Cr-rich coating layer) predicted by Pandat thermo-calculation program are as follows [9]:

1. Liquid  $\rightarrow$  Cr at 1492–1283 °C
2. Liquid  $\rightarrow$  Cr + Al<sub>2</sub>Zr at 1283–1255 °C
3. Liquid + Al<sub>2</sub>Zr  $\rightarrow$  Cr + Al<sub>3</sub>Zr at 1255 °C
4. Liquid  $\rightarrow$  Cr + Al<sub>3</sub>Zr at 1255–1238 °C
5. Liquid  $\rightarrow$  Cr + Al<sub>3</sub>Zr + Al<sub>8</sub>Cr<sub>5</sub> at 1238 °C

Cr dendrites and the Cr + AlZr eutectics should have formed upon solidification, however. The micrograph of the Cr-rich coating layer in Figure 2b reveals a somewhat different microstructure. Namely, dendritic primary Cr and AlCr phases were not observed. Additionally, in the case of the AlZr phase, it shows a dendritic morphology. This discrepancy seems to be because the growth occurred under a rapid solidification condition [10].

### 3.2. CrAl Laser-Coated Zr Alloy that Exposed to a High Temperature

Since the CrAl-coated Zr alloy is aimed to be resistant at high temperatures, the coated specimen was isothermally heated in inert atmosphere at 1100 °C for different times. Figure 3 indicates that inter-diffusion among phases in the coating layers apparently occurred after 2 h. The diffusion of aluminum appears to be significant so that the aluminum content can be detected in the Zr substrate. Generally, three distinct parts are shown: Zr-substrate, Zr-rich area, Cr-rich area (the majority of the coating layer). An intermediate area between the Zr-rich and Cr-rich area may be counted, but it was excluded as it can be regarded as a part of the Zr-rich area.

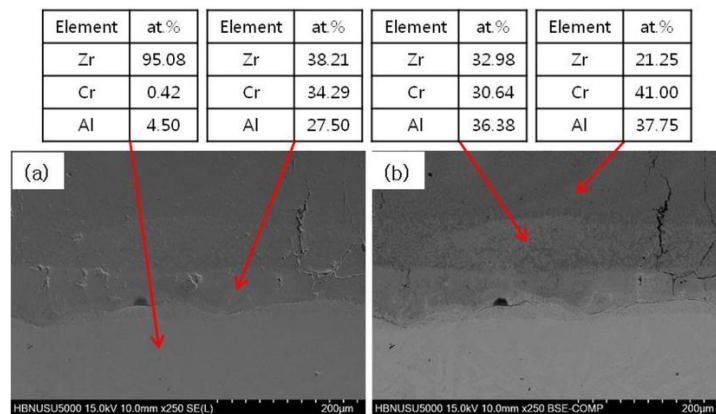


**Figure 3.** SEM-EDS analyses of laser-coated Zircaloy-4 substrate alloy after the isothermal heating at 1100 °C for 2 h in inert atmosphere: (a) bright image; (b) backscattered image.

As indicated in Figure 4, the isothermal heating clarified that the microstructure of the Zr-rich region near the substrate is composed of two regions: Zr-rich and Cr-rich. The Zr-rich area is Zr phase, and the Cr-rich area is postulated to be CrZr plus AlZr phases. Figure 5 also shows that the Cr-rich area is composed of three distinct phases. The main phase is Cr, containing about 40 at. % Al that is near the maximum solubility limit for Cr at 1100 °C. Others are Al-rich phases that include relatively large or very limited Zr content. According to the Pandat prediction and literature [9,11,12], the Al-rich phases with large Zr contents seem to be Al<sub>3</sub>Zr. Meanwhile, the Al-rich phase with a very low Zr content should be Al<sub>3</sub>Cr<sub>5</sub>. The microstructure of the coated specimens isothermally heated for 10 h was also investigated. However, the coated specimens maintained for 10 h showed similar microstructural characteristics to those of specimens held for 2 h. It is believed that the microstructure of the coating layer could be converted into near the equilibrium structure even with a holding time of just 2 h, since 1100 °C is a very high temperature.

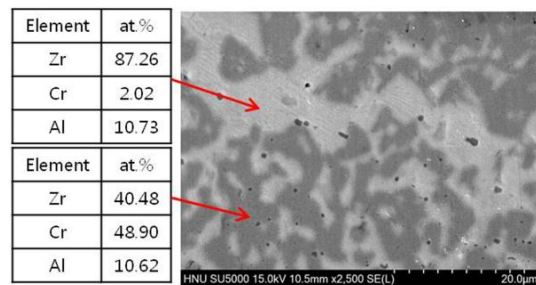


**Figure 4.** SEM-EDS analyses of Zr-rich area of CrAl-coated Zircaloy-4 alloy after the isothermal heating at 1100 °C for 2 h in inert atmosphere.

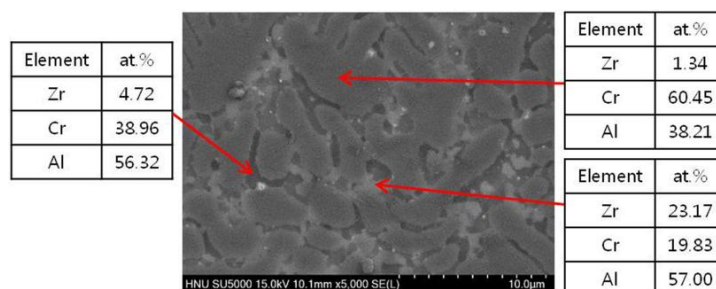


**Figure 5.** SEM-EDS analyses of CrAl coating layer on Zircaloy-4 alloy after the isothermal heating at 1100 °C for 2 h in inert atmosphere.

The chemical composition distribution as a function of depth for the CrAl-coated specimen exposed to a high temperature air is shown in Figure 6. Like Figure 3, three distinct parts are generally observed in the specimen, and it is clear that oxidation proceeded a little, only at the surface. If cracks are formed in the coating layer, they are undoubtedly undesirable, because the protective coating may be detached from the substrate. Vertically-formed cracks are supposed to be more detrimental to oxidation resistance, since oxygen ions can move easily through the cracks into the substrate. The formation of Zr oxides was observed on the Zr substrate near a vertical crack, as shown in Figure 7. However, a significant oxygen content was measured only at the top surface of CrAl coating layer in the sound region, and this suggests that the CrAl coating layer was effective in delaying the high temperature oxidation. It also appears that Al and Zr oxidize more preferentially than Cr in the coating layer. Unlike Al oxides, Zr oxides are not protective against oxidation toward the matrix at high temperatures [1,2]. Therefore, a mixing between CrAl coating layer and Zr substrate should be carefully controlled to minimize the Zr content at the top of the surface coating layer.

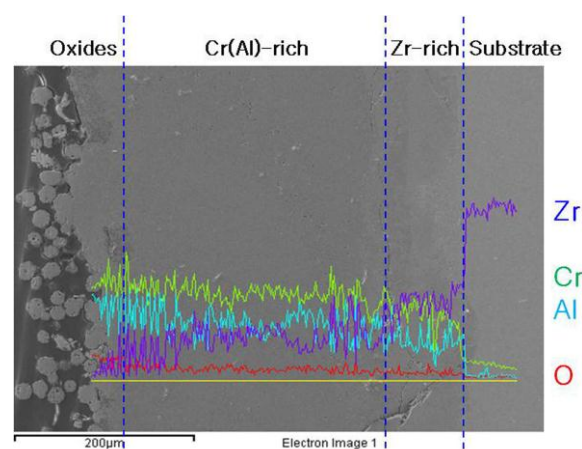


**Figure 6.** SEM micrographs with EDS profiles of the oxidized CrAl coating layer on Zircaloy-4 after isothermal heating at 1100 °C for 10 min in air.

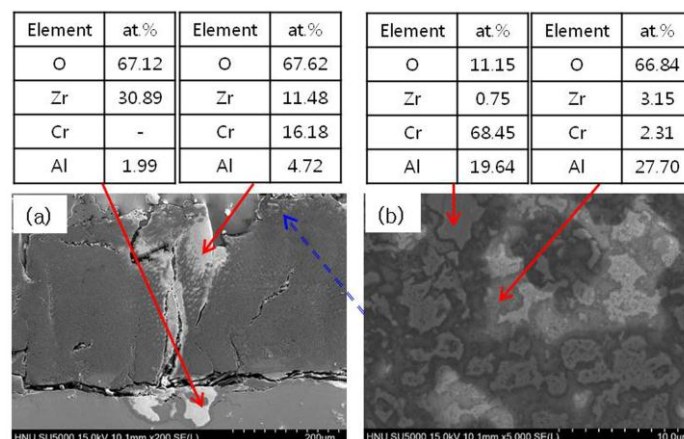


**Figure 7.** SEM-EDS analyses of laser coated Zircaloy-4 substrate alloy after isothermal heating at 1100 °C for 30 min in air: (a) near the substrate; (b) top surface of the coating layer.

### 3.3. Oxidation Behavior of CrAl Laser-Coated Zr Alloy at High Temperature

To clearly compare the oxidation resistance of CrAl coating layer with that of the Zr-incorporated CrAl layer, Cr-30 wt. % Al and Cr-30 wt. % Al-20 wt. % Zr alloy cast specimens were fabricated by vacuum arc remelting, and an oxidation test in steam at 1200 °C for 1 h was carried out. In the



case of accident, the temperature for nuclear cladding can be extremely increased, and is expected to be still under steam atmosphere. The corrosion resistance under atmosphere containing moisture can be quite different from that under dry air. Although Si and  $\text{SiO}_2$  are highly corrosion-resistant materials, they were quickly dissolved in a pressurized water condition at 360 °C in 18.9 MPa [2]. As shown in Figure 8, the coating layer without Zr possesses remarkably higher oxidation resistance than the Zr-mixed layer. Namely, much higher weight gain was observed for the Zr-containing alloy as compared to the CrAl alloy without Zr. The oxidation behavior for ZrCr30Al specimen (Zr alloy containing 30 wt. % Cr and 20 wt. % Al) was also compared for reference. Even though Cr and Al are contained in large amounts, it can be confirmed that the Zr alloy is seriously oxidized in a high temperature steam atmosphere.

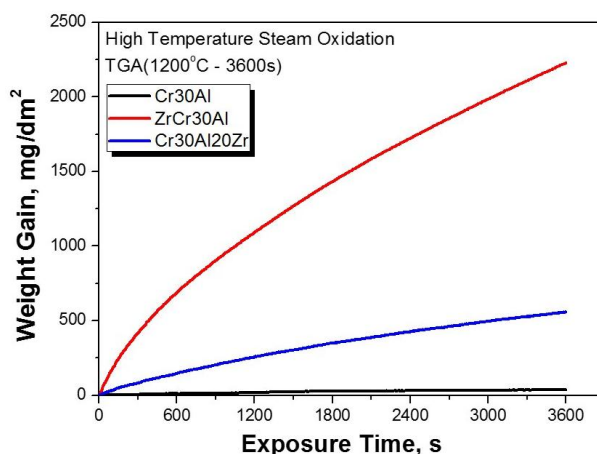


**Figure 8.** Oxidation behavior of Cr-30%Al cast alloys with and without Zr after the steam oxidation test at 1200 °C for 1 h (Zr alloy containing Cr and Al is also compared for reference).

Figure 9 indicates that a stable  $\text{Al}_2\text{O}_3$  phase is observed a lot in the surface of the Cr-30%Al alloy. It is worth mentioning that a  $\text{Cr}_2\text{O}_3$  phase was not found in that specimen. Although both  $\text{Cr}_2\text{O}_3$  and  $\text{Al}_2\text{O}_3$  phases are generally stable, the  $\text{Al}_2\text{O}_3$  phase is believed to be more stable, resulting in a continuous external  $\text{Al}_2\text{O}_3$  layer. This phenomenon has been known as transient oxidation [13]. If the content of aluminum in the coating layer is insufficient, it is considered that the  $\text{Cr}_2\text{O}_3$  is observed on the coating surface. Meanwhile, a significant amount of  $\text{ZrO}_2$  and  $\text{Al}_2\text{O}_3$  phases were found in the case of the Zr-added alloy. Since the Zr oxide is not protective, the existence of a surface  $\text{ZrO}_2$  layer should be responsible for the comparatively lower oxidation resistance.

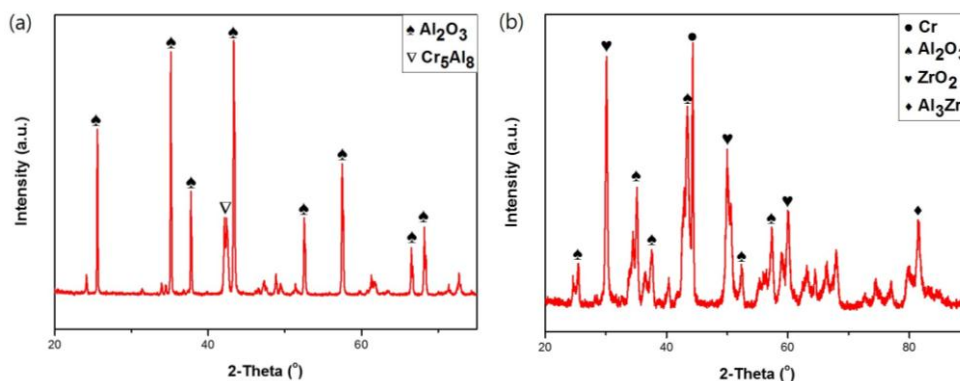


**Figure 9.** XRD analyses of cast specimens after the steam oxidation test at 1200 °C for 1 h: (a) Cr-30%Al; (b) Cr-30%Al-20%Zr alloy.

#### 4. Conclusions

It was found that a significant mixing between the CrAl layer and the Zr substrate and the formation of rapidly solidified microstructure occurred during the laser surface coating process. Inter-diffusions among the solidified phases took place when the coated specimens were isothermally heated at 1100 °C, and resulted in the formation of equilibrium phases after just 2 h. Since Zr is easily oxidized and Zr oxides are not protective against oxidation, the Zr content at the top of coating layer should be minimized to avoid deteriorated oxidation resistance.

**Acknowledgments:** This work was supported by the National Research Foundation of Korea (NRF) grant funded by Korea government (MSIP) (NRF-2012M2A8A5025822).

**Author Contributions:** J.-M.K. designed the research and wrote the manuscript with help from the other authors; T.-H.H. and I.-H.K. performed experiments; J.-M.K. and H.-G.K. analyzed the data.

**Conflicts of Interest:** The authors declare no conflict of interest.

#### References

1. Kuprin, A.S.; Belous, V.A.; Voyevodin, V.N.; Bryk, V.V.; Vasilenko, R.L.; Ovcharenko, V.D.; Reshetnyak, E.N.; Tolmachova, G.N.; Vyugov, P.N. Vacuum-arc chromium-based coatings for protection of zirconium alloys from the high temperature oxidation in air. *J. Nucl. Mater.* **2015**, *465*, 400–406. [CrossRef]
2. Kim, H.G.; Kim, I.H.; Jung, Y.I.; Park, D.J.; Park, J.Y.; Koo, Y.H. Adhesion property and high-temperature oxidation behavior of Cr-coated Zircaloy-4 cladding tube prepared by 3D laser coating. *J. Nucl. Mater.* **2015**, *465*, 531–539. [CrossRef]
3. Terrani, K.A.; Parish, C.M.; Shin, D.; Pint, B.A. Protection of zirconium by alumina- and chromia-forming iron alloys under high-temperature steam exposure. *J. Nucl. Mater.* **2013**, *438*, 64–71. [CrossRef]
4. Jin, D.; Yang, F.; Zou, Z.; Gu, L.; Zhao, X.; Guo, F.; Xiao, P. A study of the zirconium alloy protection by Cr<sub>2</sub>C<sub>2</sub>-NiCr coating for nuclear reactor application. *Surf. Coat. Technol.* **2016**, *287*, 55–60. [CrossRef]
5. Kim, J.M.; Ha, T.H.; Park, J.S.; Kim, H.G. Effect of laser surface treatment on the corrosion behavior of FeCrAl-coated TZM alloy. *Metals* **2016**, *6*, 29. [CrossRef]
6. Chen, C.; Zhang, J.; Duan, C.; Feng, X.; Shen, Y. Investigation of Cr-Al composite coatings fabricated on pure Ti substrate via mechanical alloying method: Effects of Cr-Al ratio and milling time on coating, and oxidation behavior of coating. *J. Alloy. Compd.* **2016**, *660*, 208–219. [CrossRef]
7. Gonzalez, R.O.; Gribaudo, L.M. Analysis of controversial zones of the Zr-Cr equilibrium diagram. *J. Nucl. Mater.* **2005**, *342*, 14–19. [CrossRef]
8. Kim, H.G.; Kim, I.H.; Jung, Y.I.; Park, D.J.; Park, J.Y.; Koo, Y.H. High temperature oxidation behavior of Cr-coated zirconium. In Proceedings of the LWR fuel performance meeting, Charlotte, NC, USA, 15–19 September 2013; p. 840.
9. PANDAT. CompuTherm, LLC, Madison, WI, USA. Available online: <http://www.compuTherm.com> (accessed on 13 February 2017).
10. Yue, T.M.; Xie, H.; Lin, X.; Yang, H.O. Phase evolution and dendritic growth in laser cladding of aluminium on zirconium. *J. Alloy. Compd.* **2011**, *509*, 3705–3710. [CrossRef]
11. Okamoto, H. Phase diagrams for binary alloys. In *ASM Desk Handbook*; ASM International: Materials Park, OH, USA, 2000.
12. Zhang, M.; Xu, B.; Ling, G. Preparation and characterization of  $\alpha$ -Al<sub>2</sub>O<sub>3</sub> film by low temperature thermal oxidation of Al<sub>8</sub>Cr<sub>5</sub> coating. *Appl. Surf. Sci.* **2015**, *331*, 1–7. [CrossRef]
13. Birks, N.; Meier, G.H.; Pettit, F.S. *Introduction to the High-Temperature Oxidation of Metals*; Cambridge University Press: Cambridge, UK, 2006; pp. 101–162.



© 2017 by the authors; licensee MDPI, Basel, Switzerland. This article is an open access article distributed under the terms and conditions of the Creative Commons Attribution (CC BY) license (<http://creativecommons.org/licenses/by/4.0/>).